



The advantages of data assimilation in parametric space rather than classic grid space

Solène Dealbera^{1,2}, Stéphane Raynaud³, Carlos Granero Belinchon^{1,2}, Brahim Boussidi⁴, Clément Le Goff⁴, and Pierre Tandeo^{1,2}

¹IMT Atlantique, Lab-STICC, UMR 6285, 29238, CNRS, Brest, France

²ODYSSEY Team-Project, INRIA Ifremer IMT-Atl., 35042, CNRS, Brest, France

³Shom, 29200 Brest, France

⁴LEGOS Observatoire Midi-Pyrénées, 14 avenue Édouard Belin, 31400 Toulouse

Correspondence: Solène Dealbera (solene.dealbera@imt-atlantique.fr)

Abstract. Data assimilation (DA), by merging observation and background information, is an important tool in the field of geosciences. However, in the presence of geophysical structures such as cyclones or ocean eddies, classic DA schemes in gridded space fail to properly estimate the structure properties, for example, their position and intensity. In this work, we propose a new DA scheme, in a reduced parametric space, which assimilates only the relevant parameters to describe the structures, with an application to a one-dimensional ocean eddy. Comparison of DA performed in the classic gridded field and in the parametric space is made through a series of experiments with perturbed eddy parameters. Results show that DA in the parametric space can account for the nonlinearity of the eddy parameters and preserve eddy properties. This is not the case for classic DA in the gridded space. Moreover, DA in the parametric space considerably reduces the computational cost.

1 Introduction

Data assimilation (DA) is widely used in geosciences and allows the combination of two types of information: one from a model, also known as the background, and the other from observations (Carrassi et al., 2018). The classic approach in DA consists in estimating the full state of the system, i.e., all variables of interest on a given spatial grid.

In this study, we are not interested in estimating the full state of the system, but working on specific geophysical structures (GS), such as cyclones or ocean eddies. Indeed, when sequential DA is applied to the full state in a gridded space, the analysis step often faces the problem of a mismatch between the position and shape of the observed and background GSs. The result of DA tends to alter the physical properties of GSs (Chen and Snyder, 2007). To address the issue, two main approaches have been proposed.

The first approach consists in remaining in the full state of the system, either by using non-Gaussian methods such as particle filters (Poterjoy, 2016), or by applying an a priori transformation of the background field and then apply a classic Gaussian



method such as EnKF (e.g., Ravela et al. (2007) or Ying et al. (2023), and more recently Zhen et al. (2025)). In the case of the particle filter, DA is computationally costly and struggles to handle a large state space. In the case of a transformation before the analysis stage, the cost depends on the ensemble size and the tuning of the transformation step can affect the capture of the mismatch (Feyeux et al., 2018).

25 The second approach consists in performing DA in a reduced subspace (see the review by Cheng et al. (2023)). This subspace can be constructed using statistical methods such as autoencoders or empirical orthogonal functions, but these methods struggle to represent GSs accurately (Alvera-Azcárate et al., 2025). Another kind of subspace is also possible, based on physical considerations. In that case, the GS is simplified using a simple parametric form that takes into account shape and intensity. However, to our knowledge, DA has never been investigated in this reduced parametric subspace.

30 In this study, we propose working with a DA scheme based solely on the parameters of a particular GS. We consider the case of an ocean eddy, defined by its position, radius, and amplitude. In addition to the advantage of reduced space leading to lower computational costs, this assimilation method allows us to directly estimate the expectation and covariance of the GS parameters and to preserve the properties of the GS.

In this paper, simple numerical experiments are implemented to compare the DA analysis step in a conventional gridded space with the one proposed in a reduced parametric space. The representation of the eddy and the DA methods are described in Section 2, the numerical experiments in Section 3, and the results in Section 4. Conclusions and perspectives are given in Section 5.

2 Methodology

The objective of this paper is to blend two sources of information, a background and an observation, using a basic DA algorithm.

40 We suppose that the eddy properties, hereinafter called *parameters*, have been estimated using standard detection algorithms. As we consider its one-dimensional cross-shore section, the following parameters are defined: the peak amplitude a , the peak position p and the maximal velocity radius r . Previous studies (Chelton et al., 2011) in the global ocean have shown that a Gaussian profile best fits the sea surface anomaly associated with the eddy with the function h along a longitude vector \mathbf{lon} such that

$$45 \quad h(\mathbf{lon}; a, p, r) = a \exp \left(-\frac{1}{2} \left(\frac{\mathbf{lon} - p}{r} \right)^2 \right). \quad (1)$$

Two spaces are considered for the eddy representation: the *parametric space* (noted `param`) of dimension $n=3$, corresponding to the parameters a , p , and r , and the *gridded space* (noted `grid`) of dimension m , the length of the longitude vector. h is a conversion function from the `param` to the `grid` space.

Considering background eddy parameters $\mathbf{x}^{b, \text{param}}$ and its associated surface height $\mathbf{x}^{b, \text{grid}} = h(\mathbf{lon}; \mathbf{x}^{b, \text{param}})$, we define the
 50 updated state vector:

$$\mathbf{x} = \mathbf{x}^b + \boldsymbol{\eta}^b, \quad (2)$$



with a stochastic error $\boldsymbol{\eta}^b \sim \mathcal{N}(\mathbf{0}, \mathbf{B})$. This updated state vector is related to the observation by:

$$\mathbf{y} = \mathcal{H}(\mathbf{x}) + \varepsilon, \quad (3)$$

where \mathbf{y} is the observation vector, \mathcal{H} is the observation operator, and $\varepsilon \sim \mathcal{N}(\mathbf{0}, \mathbf{R})$ is the stochastic observation error. Similarly
 55 to the background eddy, the observed eddy is first defined by its parameters $\mathbf{y}^{\text{param}}$ and their associated surface height $\mathbf{y}^{\text{grid}} = h(\mathbf{lon}; \mathbf{y}^{\text{param}})$.

In our case, since the state vector is fully observed in both spaces, the operator \mathcal{H} is the identity matrix, leading to a simple
 linear observation equation. For the sake of simplicity, we suppose that the parameters are fully independent and that the
 detection algorithm gives same values of uncertainties $\boldsymbol{\sigma}^2 = [\sigma_a^2, \sigma_p^2, \sigma_r^2]$ for the background eddy and its observation, such that
 60 the error matrices $\mathbf{B}^{\text{param}} = \mathbf{R}^{\text{param}} = \boldsymbol{\sigma}^2 \mathbf{I}_3$, where $\boldsymbol{\sigma}$ is the standard deviation.

Since the uncertainties of the surface height in the reconstructed grid space depend on the highly nonlinear parameters,
 we employ an Ensemble Optimal Interpolation (EnOI). Considering the background ensembles $\mathbf{X}^{b,\text{param}}$ and $\mathbf{X}^{b,\text{grid}} = h(\mathbf{lon}; \mathbf{X}^{b,\text{param}})$
 and the observation ensembles $\mathbf{Y}^{\text{param}}$ and $\mathbf{Y}^{\text{grid}} = h(\mathbf{lon}; \mathbf{Y}^{\text{param}})$, the EnOI scheme is the following, with
 the update of the ensemble mean

$$\overline{\mathbf{X}}^a = \overline{\mathbf{X}}^b + \mathbf{K} (\overline{\mathbf{Y}} - \overline{\mathbf{X}}^b) \quad (4)$$

and of the covariance

$$\mathbf{P}^a = (\mathbf{I} - \mathbf{K}) \mathbf{B}, \quad (5)$$

where \mathbf{K} is the Kalman gain, given by $\mathbf{K} = \mathbf{B}(\mathbf{B} + \mathbf{R})^{-1}$, where $\mathbf{B} = \text{Cov}(\mathbf{X}^b, \mathbf{X}^b)$ and $\mathbf{R} = \text{Cov}(\mathbf{Y}, \mathbf{Y})$.

The data assimilation is performed in both spaces, indicated with the superscript `param` and `grid`, and Figure 1 illustrates
 70 those two approaches.

3 Experiments

The comparison of DA in both spaces is tested with three experiments, each one illustrating the impact of a different structure
 parameter on the assimilation. Experiment #1 is performed with a different amplitude a between the background and the
 observation, while keeping the same position p and radius r , which are perfectly known. This case is referred to as the amplitude
 75 perturbation. Experiment #2 is performed with a different position p , while keeping the same amplitude a and radius r ,
 which are perfectly known. This case is referred to as the position perturbation. Experiment #3 is performed with a different
 radius r , while keeping the same amplitude a and position p , which are perfectly known. This case is referred to as the
 radius perturbation. An ensemble of 10000 members is considered both for the background and the observation. The ensemble
 members for both the background and the observation in the `param` space are generated by randomly perturbing the parameters
 80 a , p and r around $\boldsymbol{\sigma}^2$. The ensemble members in the gridded space are generated by applying Eq. (1) to the parametric ensemble.
 The Table 1 gives the parameterizations for both experiments.

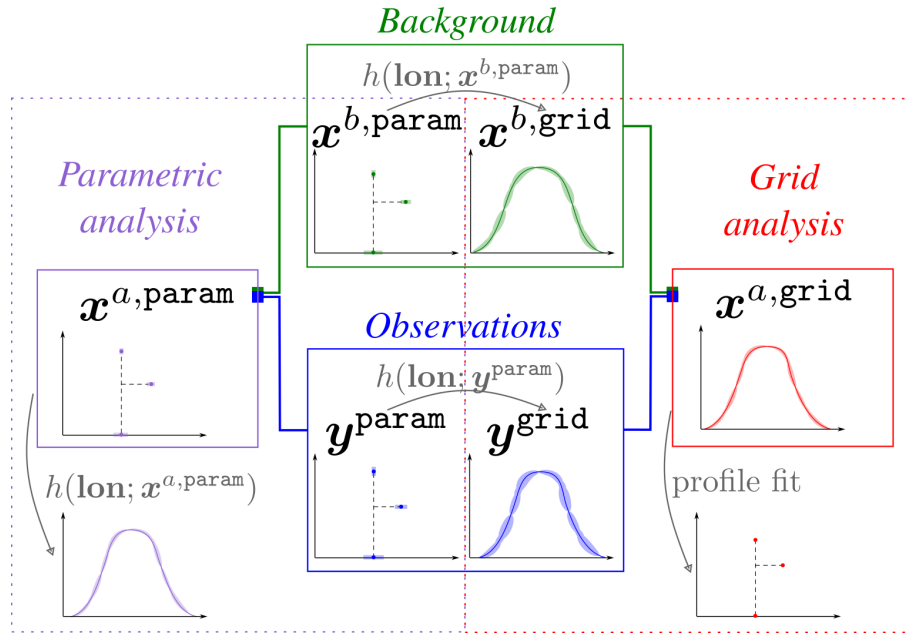


Figure 1. Schematic diagram of the data assimilation of the one-dimensional cross-shore section of an eddy in two different spaces, both parametric and gridded. The green color indicates the background, the blue color the observation, the purple color the DA in the parametric space (using amplitude, position, and radius), the red color the DA in the gridded space (using the surface height along the longitude vector).

Table 1. Values of the eddy parameters in each experiment setting.

Experiment	Eddy	Amplitude a [m]	Position p [km]	Radius r [km]
#1	Background	1.0 ± 0.5	0	7
	Observation	5.0 ± 0.5	0	7
#2	Background	1.0	-5 ± 7	7
	Observation	1.0	5 ± 7	7
#3	Background	1.0	0	7 ± 5
	Observation	1.0	0	15 ± 5

Two comparisons are performed: the reconstruction of the surface height and the estimation of the eddy parameters. To compare the surface height reconstruction, the assimilated parameters are projected into the `grid` space through Eq. (1). To evaluate the estimation of eddy parameters, the assimilated gridded products are projected into the `param` space through a Gaussian profiled fitting.

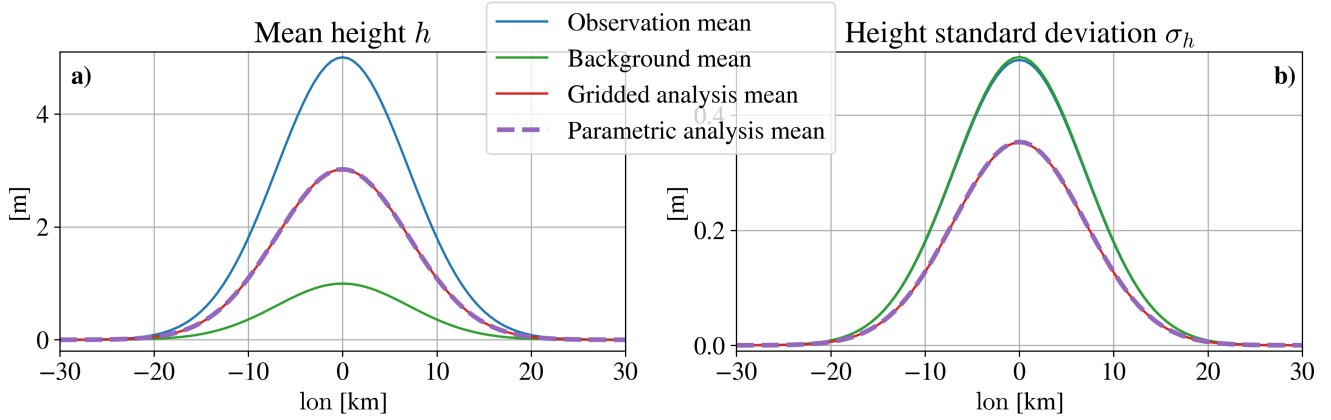


Figure 2. Results for the amplitude perturbation experiment. Left: Surface height of observed (blue) and background (green) eddy, and resulting height from gridded assimilation (red) and parametric assimilation (dashed purple) along the longitude. Right: same label for the standard deviation of surface height along the longitude.

4 Results and discussion

The surface height profiles as a function of the longitude are shown in Fig. 2, 3 and 4 for the amplitude, position and radius perturbation experiments, respectively. In Fig. 2a), we notice the same analyzed profiles for both `param` and `grid` spaces, as the exact mean of the background and observation heights. The amplitude of the analyzed eddies is estimated to be at 3.0 m, without changes in the position or the radius. Figure 2b) also shows similar results in both `param` and `grid` spaces for the estimation of the a posteriori error of the data assimilation given in Eq. (5). Those similar results between `grid` and `param` assimilation are due to the fact that amplitude is a linear parameter of the function h defined in Eq. (1).

By contrast, in Fig. 3a), the analyzed height profile in the `grid` space displays a flattened and widened shape compared to the one in the `param` space. Indeed, though the position is accurate in the gridded space, the amplitude is underestimated and the radius is overestimated (0.8 m and 9 km, respectively). This result reflects the nonlinear effect of the position p in the definition of the function h in Eq. (1). The analyzed profile in the `param` space displays similar amplitude (1.0 m) and radius (7 km) to the background and to the observation, and the position is the exact mean of the two, i.e. 0 km. In Fig. 3, the analyzed standard deviation in the `grid` space is also underestimated compared to the `param` space, which seems more realistic.

The effect of the parameters' nonlinearity is also depicted in Fig. 4a) for Experiment #3 in the case of the radius perturbation. The `grid` height analyzed profile displays a narrower peak with a wider tail compared to the `param` profile. A further analysis shows that the `grid` analyzed profile is no longer Gaussian, its slope having decreased. On the contrary, in the `param` space, the estimated radius corresponds to the mean of the observed and background radii. Moreover, the profile is still Gaussian in the `param` space. The estimated amplitude and position are accurate in both spaces and correspond to the observation and

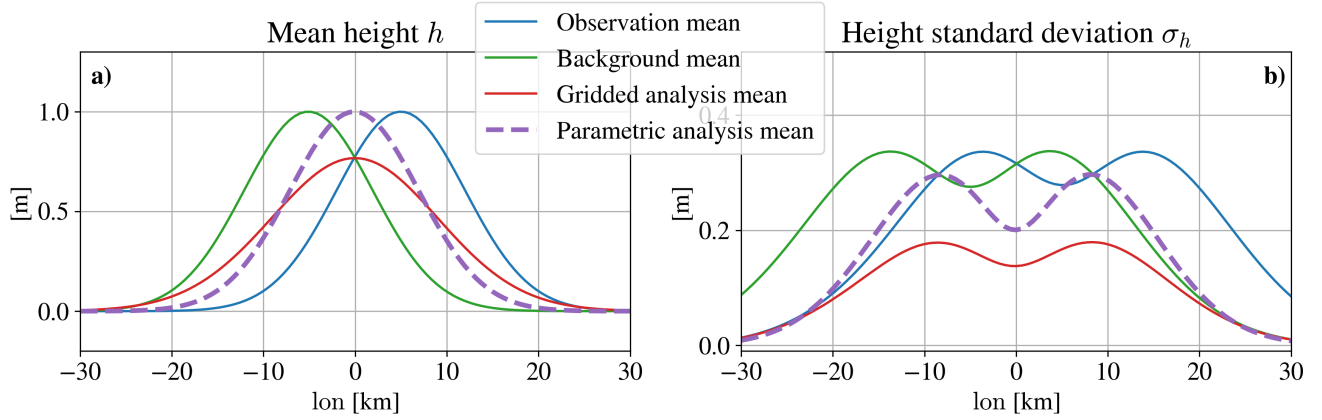


Figure 3. Results for the position perturbation experiment. Left: Surface height of observed (blue) and background (green) eddy, and resulting height from gridded assimilation (red) and parametric assimilation (dashed purple) along the longitude. Right: same label for the standard deviation of surface height along the longitude.

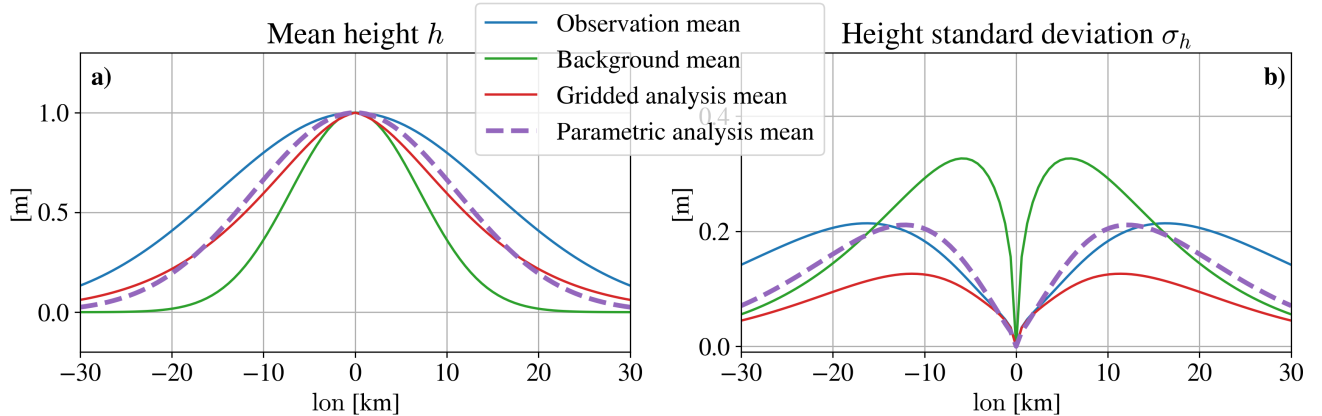


Figure 4. Results for the radius perturbation experiment. Left: Surface height of observed (blue) and background (green) eddy, and resulting height from gridded assimilation (red) and parametric assimilation (dashed purple) along the longitude. Right: same label for the standard deviation of surface height along the longitude.

background parameters. Similarly to Experiment #2, Figure 4b) shows an underestimation of the grid standard deviation compared to the param one.

By deforming the surface height profile of the eddy, the grid DA affects the dynamic properties of the reconstructed eddies. In Experiment #2, since the grid analyzed eddy has a widened and flattened surface height compared to the background and its observation, the geostrophic current field, which is proportional to the height horizontal gradient, is modified. It leads to



a reduction in the rotational velocity, therefore to an underestimation of the Eddy Kinetic Energy (EKE). The value of the total EKE is reduced by 67% compared to the value obtained with the reconstructed profile from the `param` space analyzed parameters. In Experiment #3, the decrease in the profile slope leads to smaller height gradients, hence to smaller rotational velocities and underestimated EKE. The value of the total EKE is reduced by 11% compared to the `param` value.

5 Conclusions

This paper explores DA in the parametric space of a 1D simplified ocean eddy compared to the DA in the classic gridded space. The experiments show that performing DA in the gridded space gives a good estimation of the eddy profile if only the linear parameters are perturbed, here the amplitude a . If nonlinear parameters are perturbed, here the position p and the radius r , the estimated eddy profile is deformed, with modification of the eddy parameters compared to the observed and background inputs. This impacts the quantification of dynamical properties, i.e. the kinetic energy and the geostrophic currents. Moreover, still in the gridded space, the a posteriori error is underestimated.

By contrast, DA in the parametric space shows perfect estimation of all the parameters (i.e., amplitude, position, and radius), with realistic values of a posteriori errors. Moreover, performing DA in the `param` space drastically reduces the dimensions of the system, which is limited by the number of selected parameters and not by the resolution of the grid. Finally, it does not need an ensemble scheme, while performing DA in the `grid` requires a minimum of 25 members to avoid degradation of eddy properties. To conclude, DA in `param` space is useful in the context of well-defined geophysical structures, such as the eddies, cyclones, algal blooms, wildfires, and rainfronts, for instance.

Perspectives of work is to apply this new DA scheme in the parametric space within an operational framework for mesoscale ocean eddy forecasting. In this case, a machine learning model will be required to emulate the temporal dynamics of the eddy parameters. Moreover, satellite observations will provide location and shape parameters of the eddies.

Code availability. The code used for the Experiments is available there: <https://gitlab.imt-atlantique.fr/s24dealb/param-grid-1d-eddy>

Author contributions. SD developed the code and performed the experiments and prepared the manuscript with contributions from co-authors, SR proposed the research topic, provided knowledge and background, performed the seminal experiments, and offered mentorship throughout this research, PT and CGB provided knowledge and assistance during code development, CL and BB helped with the redaction of the paper.

Acknowledgements. This study was carried out as part of the PTD PROTEVS2, project financed by the French Ministry of Defense / DGA and led by Shom.



References

- Alvera-Azcárate, A., Van Der Zande, D., Barth, A., Dille, A., Massant, J., and Beckers, J.-M.: Generation of super-resolution gap-free ocean colour satellite products using data-interpolating empirical orthogonal functions (DINEOF), *Ocean Science*, 21, 787–805, <https://doi.org/10.5194/os-21-787-2025>, 2025.
- 140 Carrassi, A., Bocquet, M., Bertino, L., and Evensen, G.: Data assimilation in the geosciences: An overview of methods, issues, and perspectives, *WIREs Climate Change*, 9, e535, <https://doi.org/10.1002/wcc.535>, 2018.
- Chelton, D. B., Schlax, M. G., and Samelson, R. M.: Global observations of nonlinear mesoscale eddies, *Progress in Oceanography*, 91, 167–216, <https://doi.org/10.1016/j.pocean.2011.01.002>, 2011.
- Chen, Y. and Snyder, C.: Assimilating Vortex Position with an Ensemble Kalman Filter, *Monthly Weather Review*, 135, 1828–1845, <https://doi.org/10.1175/MWR3351.1>, 2007.
- 145 Cheng, S., Quilodrán-Casas, C., Ouala, S., Farchi, A., Liu, C., Tandeo, P., Fablet, R., Lucor, D., Iooss, B., Brajard, J., Xiao, D., Janjic, T., Ding, W., Guo, Y., Carrassi, A., Bocquet, M., and Arcucci, R.: Machine Learning With Data Assimilation and Uncertainty Quantification for Dynamical Systems: A Review, *IEEE/CAA Journal of Automatica Sinica*, 10, 1361–1387, <https://doi.org/10.1109/JAS.2023.123537>, 2023.
- 150 Feyeux, N., Vidard, A., and Nodet, M.: Optimal transport for variational data assimilation, *Nonlinear Processes in Geophysics*, 25, 55–66, <https://doi.org/10.5194/npg-25-55-2018>, 2018.
- Poterjoy, J.: A Localized Particle Filter for High-Dimensional Nonlinear Systems, *Monthly Weather Review*, 144, 59–76, <https://doi.org/10.1175/MWR-D-15-0163.1>, 2016.
- Ravela, S., Emanuel, K., and McLaughlin, D.: Data assimilation by field alignment, *Physica D: Nonlinear Phenomena*, 230, 127–145, <https://doi.org/10.1016/j.physd.2006.09.035>, 2007.
- 155 Ying, Y., Anderson, J. L., and Bertino, L.: Improving Vortex Position Accuracy with a New Multiscale Alignment Ensemble Filter, *Monthly Weather Review*, 151, 1387–1405, <https://doi.org/10.1175/MWR-D-22-0140.1>, 2023.
- Zhen, Y., Resseguier, V., and Chapron, B.: Alignment of geophysical fields: A differential geometry perspective, *Physica D: Nonlinear Phenomena*, 483, 134 997, <https://doi.org/10.1016/j.physd.2025.134997>, 2025.